

Transport properties of $Tl_2Ba_2CaCu_2O_8$ microbridges on a low-angle step substrate

Sheng-Hui Zhao(赵生辉), Wang-Hao Tian(田王昊), Xue-Lian Liang(梁雪连), Ze He(何泽), Pei Wang(王培), Lu Ji(季鲁), Ming He(何明), and Hua-Bing Wang(王华兵)

Citation: Chin. Phys. B, 2021, 30 (**6**): 060308. DOI: 10.1088/1674-1056/abec35
Journal homepage: http://cpb.iphy.ac.cn; http://iopscience.iop.org/cpb

What follows is a list of articles you may be interested in

Dynamics of bright soliton in a spin-orbit coupled spin-1 Bose-Einstein condensate

Hui Guo(郭慧), Xu Qiu(邱旭), Yan Ma(马燕), Hai-Feng Jiang(姜海峰), and Xiao-Fei Zhang(张晓斐)
Chin. Phys. B, 2021, 30 (**6**): 060310. DOI: 10.1088/1674-1056/abf34a

Dynamical stability of dipolar condensate in a parametrically modulated one-dimensional optical lattice

Ji-Li Ma(马吉利), Xiao-Xun Li(李晓旬), Rui-Jin Cheng(程瑞锦), Ai-Xia Zhang(张爱霞), and Ju-Kui Xue(薛具奎)
Chin. Phys. B, 2021, 30 (**6**): 060307. DOI: 10.1088/1674-1056/abd746

Spin-orbit-coupled spin-1 Bose-Einstein condensates confined in radially periodic potential

Ji Li(李吉), Tianchen He(何天琛), Jing Bai(白晶), Bin Liu(刘斌), and Huan-Yu Wang(王寰宇)
Chin. Phys. B, 2021, 30 (**3**): 030302. DOI: 10.1088/1674-1056/abc53e

Lattice configurations in spin-1 Bose–Einstein condensates with the SU(3) spin–orbit coupling

Ji-Guo Wang(王继国)†, Yue-Qing Li(李月晴), and Yu-Fei Dong(董雨菲)
Chin. Phys. B, 2020, 29 (**10**): 100304. DOI: 10.1088/1674-1056/abab72

Interference properties of two-component matter wave solitons

Yan-Hong Qin(秦艳红), Yong Wu(伍勇), Li-Chen Zhao(赵立臣), Zhan-Ying Yang(杨战营)
Chin. Phys. B, 2020, 29 (**2**): 020303. DOI: 10.1088/1674-1056/ab65b7

Transport properties of $Tl_2Ba_2CaCu_2O_8$ microbridges on a low-angle step substrate

Sheng-Hui Zhao(赵生辉)[1], Wang-Hao Tian(田王昊)[2], Xue-Lian Liang(梁雪连)[1], Ze He(何泽)[1], Pei Wang(王培)[3], Lu Ji(季鲁)[1,4,†], Ming He(何明)[1], and Hua-Bing Wang(王华兵)[2,‡]

[1] *College of Electronic Information and Optical Engineering, Nankai University, Tianjin* 300350, *China*
[2] *Research Institute of Superconductor Electronics, Nanjing University, Nanjing* 210093, *China*
[3] *Beijing Institute of Radio Measurement, Beijing* 100854, *China*
[4] *Key Laboratory of Photoelectronic Thin Film Devices and Technology of Tianjin, Tianjin* 300350, *China*

(Received 27 January 2021; revised manuscript received 25 February 2021; accepted manuscript online 5 March 2021)

Tl-based superconducting devices have been drawn much attention for their high transition temperature (T_c), which allow the high temperature superconductors (HTS) devices to operate at temperature near 100 K. The realization of Tl-based devices will promote the research and application of HTS devices. In this work, we present transport properties of $Tl_2Ba_2CaCu_2O_8$ (Tl-2212) microbridges across a low-angle step on $LaAlO_3$ (LAO) substrate. We experimentally demonstrate intrinsic Josephson effects (IJEs) in Tl-2212 films by tailoring the geometry, i.e., reducing the width of the microbridges. In the case of a 1 μm width microbridge, in addition to the observation of voltage branches and remarkable hysteresis on the current–voltage (I–V) characteristics, the temperature dependence of differential resistance shows a finite resistance above 60 K when the bias current is below the critical current. For comparison, the wider microbridges are also investigated, exhibiting a highly critical current but do not showing obvious IJEs.

Keywords: high temperature superconductors, Tl-2212, intrinsic Josephson effects, transport properties

PACS: 03.75.Lm, 74.25.F– **DOI:** 10.1088/1674-1056/abec35

1. Introduction

The high transition temperature (high-T_c) cuprate superconductors, most of which are anisotropic compounds, have layered crystal structures to form natural superconducting-blocking-superconducting trilayer sandwich structures repeatedly.[1,2] Their layered crystal structure leads to the current transport via tunneling, which is dominated by intrinsic Josephson effect (IJE). Kleiner and co-workers[3] showed the intrinsic Josephson effects in $Bi_2Sr_2CaCu_2O_8$ (BSCCO), $(Pb_yBi_{1-y})_2Sr_2CaCu_2O_8$ (PBSCCO), and $Tl_2Ba_2Ca_2Cu_3O_8$ (Tl-2223) compounds. The I–V characteristics of intrinsic Josephson junction (IJJ) exhibited both clear hysteresis and multiple branches, indicating a series connection of highly capacitive junctions. BSCCO intrinsic Josephson junctions have been extensively studied[4–6] as terahertz (THz) emitters.[7–14] In BSCCO IJJ stacks, superconducting CuO_2 planes alternating with insulating SrO and BiO layers can realize vertical c-axis transport. This natural layered structure can be applied to generate electromagnetic radiation in the terahertz regime. Additionally, it is very convenient to fabricate IJJs by growing Tl-based films on a vicinal cut substrate. Tl-2212 has an operating temperature over 100 K,[15] which is much higher than that of BSCCO and $YBa_2Cu_3O_{7-\delta}$ (YBCO). Intrinsic Josephson effects and other superconducting properties of Tl-2212 IJJs were mostly investigated on misaligned substrate,[16–28] in which films were grown epitaxially on the substrate with the same misalignment angle. In this structure, the copper oxide planes of Tl-based films create a misaligned angle with respect to the substrate surface, the superconducting current can then flow through the inter-plane along the c-axis of the sample films according to the experimental design.

Alternatively, to exploit c-axis transport, superconducting films can be deposited on a substrate into which a step has been etched. Wang *et al.* successfully fabricated IJJs in oxygen-deficient YBCO films on a low-angle $SrTiO_3$ step substrate.[29,30] Several studies[31,32] indicated that Tl-based superconducting microbridges fabricated on substrates with high step angles (usually 60°–75°) exhibited intrinsic Josephson effects, whereas microbridges on substrates with step angles lower than this interval did not show intrinsic Josephson effects due to the flux-flow effects. Some experts have different opinions on this conclusion. Yoshikawa *et al.* reported that both types of step-edge junctions or IJJs can be shown on a step substrate of the same angle (about 28°), which depends on the height of the steps.[33,34] The relationship between the step angle and the type of junctions needs to be verified by further experiments. More studies are essential to provide evidence for this field.

In this work, we use conventional photolithography, together with focused ion beam (FIB) direct-write lithography

†Corresponding author. E-mail: luji@nankai.edu.cn
‡Corresponding author. E-mail: hbwang@nju.edu.cn

© 2021 Chinese Physical Society and IOP Publishing Ltd

to fabricate superconducting microbridges on LAO step substrates. With our improved two-step method,[35,36] we present fabrication and electrical transport characterization of intrinsic Josephson junctions in Tl-2212 superconducting microbridges on a step substrate. We investigate the current–voltage characteristics of superconducting microbridges at different temperatures. We also discuss the features of IJEs, i.e., hysteresis structures and voltage jumps, in current-biased Tl-2212 microbridges.

2. Experimental method

At first, LAO substrate was etched with Ar-ion milling through a photolithography defined mask. The modified substrate has a very smooth step with the angle of $\sim 30^\circ$ measured with an atomic force microscopy (AFM). Tl-2212 films were then deposited on LAO step substrates by an improved two-step method, including dc magnetron sputtering and post annealing. This method can maintain the vapor-solid equilibrium during the formation of Tl-2212 phase crystals without adding any additional Tl sources and the uniformity of Tl-2212 films was greatly improved.[35] Besides, x-ray diffraction (XRD) was used for observing Tl-2212 phase in the film, and the scanning electron microscope (SEM) image of the Tl-2212 film is shown in Fig. 1(a). After that, microbridges were defined using standard photolithography, and pattern transfer to the Tl-2212 thin films was achieved by Ar^+ beam etching. Three microbridges with different widths, 4 μm (named sample N1, $T_{c0} = 102$ K), 6 μm (named sample N2, $T_{c0} = 105$ K), and 10 μm (named sample N3, $T_{c0} = 105$ K), were fabricated on the same sample film. Figure 1(b) provides a SEM diagram of a sample microbridge. Au wires were glued onto the electrode contact with silver conductive adhesive for better electrical contact, and transport measurements were performed with a four-point method, as shown in Fig. 1(c).

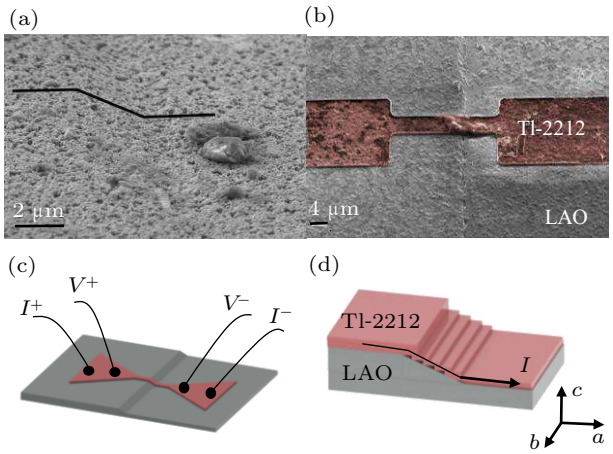


Fig. 1. (a) SEM image of the film on step substrate, black solid lines are guides for the eyes indicating the step on the substrate. (b) False-color SEM image of a typical 4-μm-wide microbridge. (c) Schematic of four-point measurement setup. (d) Schematic diagram of step growth of intrinsic Josephson junctions.

DC current source was used for biasing the samples and the voltage across the bridge was measured via a low-noise amplifier. Figure 1(d) illustrates the schematic of the film growth on a step substrate, black solid line indicates the current direction when applied a biased current in the film.

3. Results and discussion

We firstly investigated the transport properties of samples N1, N2, and N3. The *I*–*V* characteristics of sample N1 measured at 50 K are presented in Fig. 2(a). By ramping the bias current up and down, some voltage jumps appear on the *I*–*V* curve. Besides, several junctions switch from resistance state to zero voltage state along the hysteretic path when decreasing the bias current. These characteristics are typical features of IJEs for serial arrays of intrinsic Josephson junctions.

To further obtain a clear insight into the intrinsic Josephson effects, the *I*–*V* curves of sample N1 were measured with microwave irradiation. Figure 2(b) shows the *I*–*V* curves under microwave irradiation (27.1 GHz) at temperatures 50 K and 80 K. As can be seen, the current upturns appear when the microwave power is strong enough. Besides, the microwave frequency 27.1 GHz is much lower than the plasma frequency of Tl-2212 IJJs (about in THz band), which is hardly obtained in the experiments. Therefore, the phase lock between junctions is unstable in our experiment and the microwave induced steps have not been observed.[29] It should be mentioned that the current upturns in Fig. 2(b) are typical characteristics of intrinsic Josephson junctions, which are similar to the results in YBCO film[29] and BSCCO single crystal.[37,38]

To have a better understanding on the effect of microbridge width on the IJEs, we performed a number of additional characterization experiments. Figure 2(c) shows the *I*–*V* curves of the sample N2 at different temperatures from 45 K to 95 K. Figure 2(d) presents the *I*–*V* characteristics of N2 at 45 K. Compared with the *I*–*V* curves of N1, there are few voltage jumps, and the amplitude of the hysteresis is small on the *I*–*V* curves of N2. We attribute this phenomenon to the shunted resistance, induced by the defects in the microbridge, partially bypassing the current. As the bath temperature further increases, the voltage jumps and hysteresis structures apparently fade away.

Figure 3 shows a typical *I*–*V* curve of sample N3 measured at different temperature. As can be seen, hysteresis structures do not appear, but several voltage jumps can be seen on the *I*–*V* curves of sample N3 at 5 K in Fig. 3. Additionally, we see a large voltage jump (about 70 mV) on the *I*–*V* curves, which may be caused by the appearance of hotspot overheating in such high bias current. As shown in the inset of Figure 3, critical current I_c of sample N3 is much higher than that of samples N1 and N2 at the same bath temperature. By considering characteristics of polycrystalline thin film, it

can be naturally considered that this may result from the existence of a large number of non-*c*-axis crystal grains. Because the Tl-based film cannot be prepared by an *in-situ* method, the crystallization of the films in the post annealing process is accomplished in a dynamic balance of Tl_2O vapor pressure. Inevitably, comparing with YBCO and BSCCO, Tl-based films have much more defects. Therefore, as the width of the microbridge increases, these defects shorten the IJJ junctions along the *c*-axis direction of Tl-2212 films, resulting in a large I_c values in sample N3. And the *I*–*V* curves of sample N3 are similar to those of normal superconducting microbridges, and do not feature any IJEs at the same bath temperature range (40–90 K).

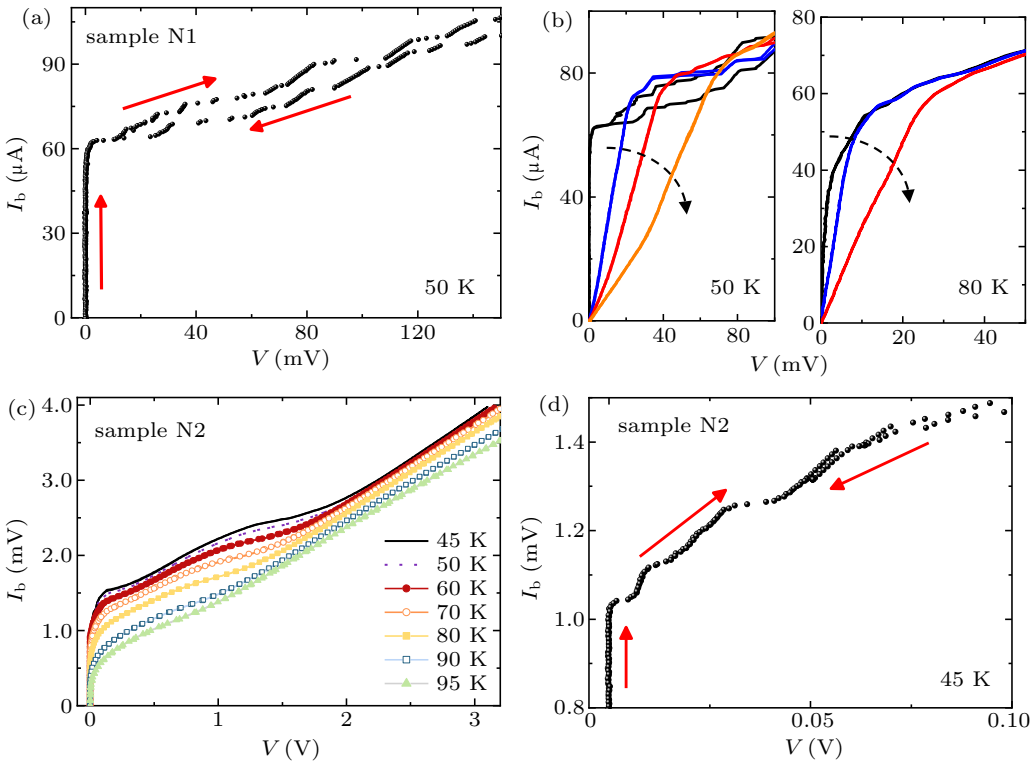


Fig. 2. (a) Current–voltage curves for sample N1 measured at temperature of 50 K. (b) The *I*–*V* curves of sample N1 under 27.1 GHz microwave irradiation at 50 K and 80 K; the dashed arrows indicate microwave power become lager. (c) The *I*–*V* curves of sample N2 measured at different temperatures from 45 K to 95 K. (d) Voltage jumps and small hysteresis measured at 45 K. Solid arrows in (a) and (d) indicate the sweeping direction of the current.

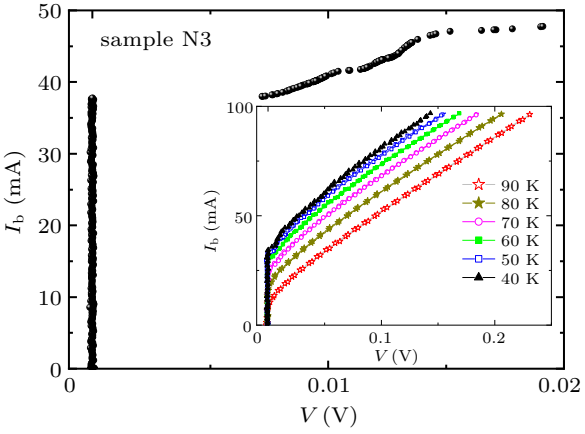


Fig. 3. Current–voltage characteristics of sample N3 at 5 K, inset shows a series of *I*–*V* curves of sample N3 measured from 40 K to 90 K in steps of 10 K.

From the data discussed above, the characteristics of IJJs in the *c*-direction of Tl-2212 films are possibly concealed with the increment of defect-induced lattice mismatch. Based on this point of view, as the width of the bridge becomes wider, the critical current becomes larger. Besides, the results of sample N1 show hysteresis structures and voltage branches on the *I*–*V* curves, which are the typical characters of intrinsic Josephson effects. Whereas no hysteresis structures but only a few voltage jumps are observed in sample N3, indicating that enlarging the width of the microbridges may weaken the characteristics of IJJs. On the contrary, narrow width of the microbridges is favorable to the formation of IJJs, which will be discussed in the following.

Due to the degradation in the microbridge (width less than 4 μm) from 200-nm-thick Tl-2212 films, we fabricated a 1-μm-wide microbridge S1 in the 500-nm-thick Tl-2212 film to further illustrate the mechanism in Tl-2212 IJJs. The patterning of narrower microbridge was accomplished by FIB direct-write technique. A focused Ga^+ beam was scanned across the 6-μm-wide superconducting bridge to mill the bridge to a width of 1 μm. The critical temperatures are 100 K ($T_c^{10\%}$) and 60 K (T_{c0}).

Figure 4(a) shows the measured *I*–*V* curves of sample S1 at different bath temperatures. In Fig. 4(b), the *I*–*V* charac-

teristics demonstrate clear multiple branches with a significant hysteresis by ramping the bias current up and down repeatedly, suggesting that our IJJs made of Tl-2212 thin films on step substrate exhibit clear *c*-axis transport properties. As shown in Fig. 4(b), when the bias current is ramped from zero, IJJs are initially in their zero-voltage state. When the current is increased to about 12.5 μA, the critical current of the weakest junction is reached and this junction switches to its resistance state. Upon further increase of the bias current, more voltage jumps appear on the *I*–*V* curves. While the junctions switch from the resistance states to the zero-voltage states individually at different return currents when the bias current is decreased. In this way, multiple branches can be traced out on the *I*–*V* curves. Normal resistances (R_n) are constant from 5 K to 30 K and have a sharp change when the bath temperature rises up to 40 K, corresponding to the large voltage jumps. It should be noticed that R_n of sample S1 measured at 40 K is larger than that at other temperatures. We believe that this may be caused by a series of IJJs switching to the resistive state directly from the superconducting state.

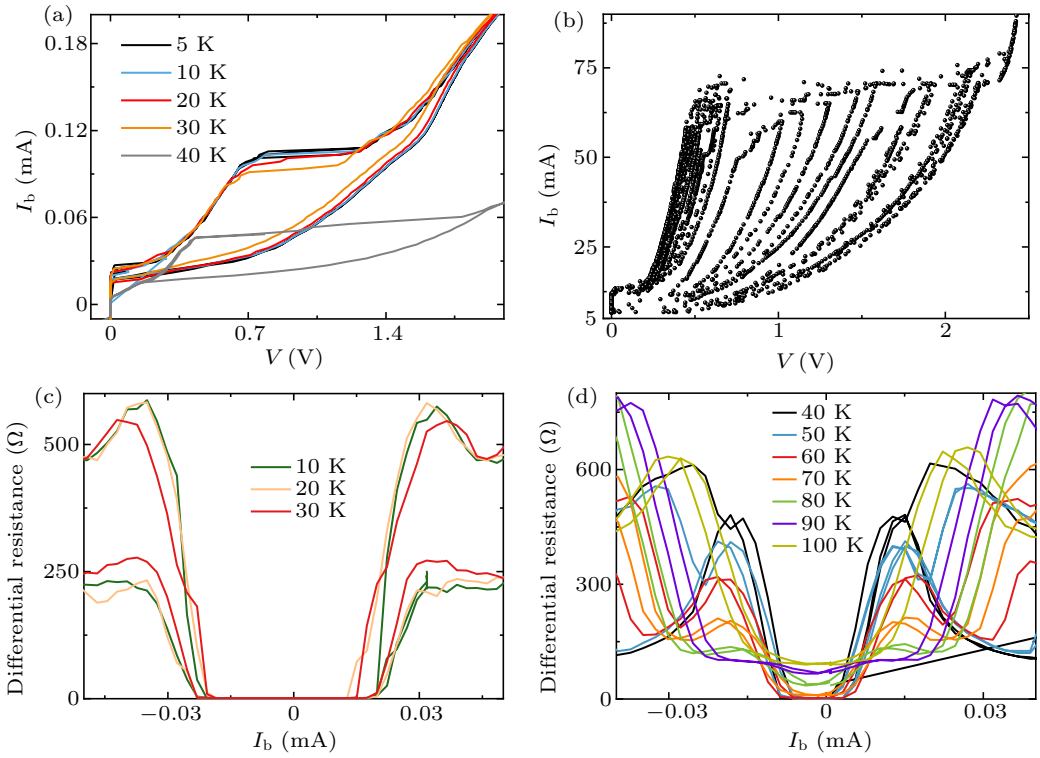


Fig. 4. (a) Back-and-forth *I*–*V* curves of sample S1 measured at 5 K and 10 K to 40 K with an increment of 10 K. (b) The voltage jumps and hysteresis in *I*–*V* curves measured at 5 K. (c) Differential resistance dV/dI versus the bias current I_b for temperatures 10 K, 20 K, and 30 K. (d) Differential resistance dV/dI versus I_b for temperatures from 40 K to 100 K in 10 K increments.

Furthermore, we measured the differential resistance using low-frequency techniques. Figures 4(c) and 4(d) plot the detailed variation of the differential resistance (dV/dI) versus bias current I_b, while sweeping bias current I_b from negative to positive current. Differential resistance peaks persist in a wide temperature range from 5 K up to 100 K. Unlike the tunnel junctions made from conventional superconductors, the decreasing of differential resistance after the first peak is a common occurrence in HTS tunnel junctions.[39] The superconducting energy gap is not available due to the unknown numbers of IJJs at different bath temperatures. It should be mentioned that, at bath temperature above 60 K, the junctions exhibit some finite resistance. And this finite resistance increases as the bath temperature increases, as plotted in Fig. 4(d). While its exact origin is not clear at this stage, we surmise that the resistance may be caused by a lack of coherent Josephson transport in a series of IJJs. These results together with the *I*–*V* curves suggest that the IJJs are formed in Tl-2212 microbridge.

In terms of relationship between the microbridge width and IJEs, we observe more obvious IJEs characteristics in a smaller width of bridge. From the result, the narrower width of the microbridge seems to have enhanced the intrinsic Josephson effects. The width scale of the superconducting bridge in the range of nanometers will be studied in the future with the help of FIB. And the measurement of such a nanobridge will be of great interest.

4. Conclusion

To conclude, using an improved two-step method we present the realization of a series of Tl-2212 intrinsic Josephson junctions on a step substrate. By varying the width of the microbridge, we observe the intrinsic Josephson effect in the narrow bridge, and it fades away as the bridge becomes wider.

We attribute this to the current bypassing of IJJs and flowing through lattice-induced defects of the film. Our results indicate that the width of the microbridge is crucial to obtain *c*-axis intrinsic Josephson junctions. Besides, the dependence of step angle and height on Josephson junction type deserves future research.

References

[1] Kleiner R 1997 *J. Low. Temp. Phys.* **106** 453
[2] Kleiner R and Wang H B 2019 *Fundamentals and Frontiers of the Josephson Effect*, Tafuri F ed. (Cham: Springer International Publishing) pp. 367–454
[3] Kleiner R and Muller P 1994 *Phys. Rev. B* **49** 1327
[4] Rudau F, Tsujimoto M, Gross B, Judd T E, Wieland R, Goldobin E, Kinev N, Yuan J, Huang Y, Ji M, Zhou X J, An D Y, Ishii A, Mints R G, Wu P H, Hatano T, Wang H B, Koshelets V P, Koelle D and Kleiner R 2015 *Phys. Rev. B* **91** 104513
[5] Rudau F, Wieland R, Langer J, Zhou X J, Ji M, Kinev N, Hao L Y, Huang Y, Li J, Wu P H, Hatano T, Koshelets V P, Wang H B, Koelle D and Kleiner R 2016 *Phys. Rev. Appl.* **5** 044017
[6] Liu F, Lin S Z and Hu X 2013 *Supercond. Sci. Technol.* **26** 025003
[7] Borodianskyi E A and Krasnov V M 2017 *Nat. Commun.* **8** 1742
[8] Zhang H L, Wieland R and Chen W, *et al.* 2019 *Phys. Rev. Appl.* **11** 044004
[9] Elarabi A, Yoshioka Y, Tsujimoto M and Kakeya I 2017 *Phys. Rev. Appl.* **8** 064034
[10] Tsujimoto M, Doi T, Kuwano G, Elarabi A and Kakeya I 2017 *Supercond. Sci. Technol.* **30** 064001
[11] Wang H B, Guenon S, Gross B, Yuan J, Jiang Z G, Zhong Y Y, Grunzweig M, Iishi A, Wu P H, Hatano T, Koelle D and Kleiner R 2010 *Phys. Rev. Lett.* **105** 057002
[12] Wang H B, Guenon S, Yuan J, Iishi A, Arisawa S, Hatano T, Yamashita T, Koelle D and Kleiner R 2009 *Phys. Rev. Lett.* **102** 017006
[13] Uchida T, Kimura W, Nakajima K, Tachiki T and Uchida T 2018 *IEEE Trans. Appl. Supercond.* **28** 1
[14] Kashiwagi T, Yuasa T, Tanabe Y, Imai T, Kuwano G, Ota R, Nakamura K, Ono Y, Kaneko Y, Tsujimoto M, Minami H, Yamamoto T, Klemm R A and Kadowaki K 2018 *J. Appl. Phys.* **124** 033901
[15] Zhao S H, Tian W H, Zhang X, Liang X L, He Z, Qi Z D, Wang P, Ji L, He M and Wang H B 2020 *Supercond. Sci. Technol.* **33** 075006
[16] Chana O S, Kuzhakhmetov A R, Warburton P A, Hyland D M C, Dew-Hughes D, Grovenor C R M, Kinsey R J, Burnell G, Booij W E, Blamire M G, Kleiner R and Müller P 2000 *Appl. Phys. Lett.* **76** 3603
[17] Yan S I, Fang L, Si M S and Wang J 1997 *J. Appl. Phys.* **82** 480
[18] Chana O S, Hyland D M C, Kinsey R J, Booij W E, Blamire M G, Grovenor C R M, Dew-Hughes D and Warburton P A 1999 *Physica C* **326–327** 104
[19] Mans M, Schneidewind H, Büenfeld M, Schmidl F and Seidel P 2006 *Phys. Rev. B* **74** 214514
[20] Wang P, Fan B, Wang Z, Xie W, Zhao X J, Zhang X, Ji L, He M, Fang L and Yan S L 2012 *J. Supercond. Nov. Magn.* **25** 1427
[21] Wang P, Xie W, Hu L, Liu X, Zhao X J, He M, Ji L, Zhang X and Yan S L 2013 *Chin. Phys. B* **22** 57402
[22] Hu L, Wang P, Xie W, Liu X, Zhao X J, He M, Ji L, Zhang X and Yan S L 2014 *J. Supercond. Nov. Magn.* **27** 353
[23] Warburton P A, Kuzhakhmetov A R, Burnell G, Blamire M G and Schneidewind H 2003 *Phys. Rev. B* **67** 184513
[24] Warburton P A, Kuzhakhmetov A R, Burnell G, Blamire M G, Koval Y, Franz A, Muller P and Schneidewind H 2005 *IEEE Trans. Appl. Supercond.* **15** 237
[25] Chana O S, Kuzhakhmetov A R, Hyland D M C, Dew-Hughes D, Grovenor C R M, Koval Y, Kleiner R, Müller P and Warburton P A 2001 *Physica C* **362** 265
[26] Warburton P A, Chana O S, Kuzhakhmetov A R, Hyland D M C, Dew-Hughes D, Grovenor C R M, Koval Y and Muller P 2001 *IEEE Trans. Appl. Supercond.* **11** 300
[27] Warburton P A, Kuzhakhmetov A R, Chana O S, Burnell G, Blamire M G, Schneidewind H, Koval Y, Franz A, Müller P, Hyland D M C, Dew-Hughes D, Wu H and Grovenor C R M 2004 *J. Appl. Phys.* **95** 4941
[28] Warburton P A 2007 *Supercond. Sci. Technol.* **20** S14
[29] Wang H B, Chen J, Tachiki T, Mizugaki Y, Nakajima K and Yamashita T 1999 *J. Appl. Phys.* **85** 3740
[30] Wang H B, Chen J, Nakajima K, Yamashita T, Wu P H, Nishizaki T, Shibata K and Kobayashi N 2000 *Phys. Rev. B* **61** R14948
[31] Veith M, Eick T, Brodkorb W, Manzel M, Bruchlos H, Köhler T, Schmidt H G, Steinbeiss E, Fuchs H J, Schlenga K, Hechtfischer G and Müller P 1996 *J. Appl. Phys.* **80** 3396
[32] Schlenga K, Kleiner R, Hechtfischer G, Mossle M, Schmitt S, Muller P, Helm C, Preis C, Forsthofer F, Keller J, Johnson H L, Veith M and Steinbeiss E 1998 *Phys. Rev. B* **57** 14518
[33] Yoshikawa S, Nemoto M, Shimaoka K, Niki K, Yoshida I and Yoshisato Y 1997 *IEEE Trans. Appl. Supercond.* **7** 3013
[34] Yoshikawa S, Nemoto M, Shimaoka K, Yoshida I and Yoshisato Y 1997 *Physica C* **293** 44
[35] Xu T D, Xing J, Wang L T, Zhang J L, Zhao S H, Xiong Y, Zhao X J, Ji L, Zhang X and He M 2018 *Chin. Phys. B* **27** 057403
[36] Ji L, Liang X L, He K Y, Xing J, Xue T, Xu T D, Wang L T, Zhang S F, Zhang X, He Z, He M, Zeng C, Yan S L and Feng M 2019 *Ceram. Int.* **45** 24635
[37] Oya G, Hashimoto T and Irie A 2006 *Supercond. Sci. Technol.* **19** S191
[38] Latyshev Y I, Gaifullin M B, Yamashita T, Machida M and Matsuda Y 2001 *Phys. Rev. Lett.* **87** 247007
[39] Cybart S A, Cho E Y, Wong T J, Wehlin B H, Ma M K, Huynh C and Dynes R C 2015 *Nat. Nanotech.* **10** 598